# Corrosion Behaviors of Structural Materialsin High Temperature S-CO$_2$ Environments

## Ho Jung Lee, Hyunmyung Kim, and Changheui Jang [†]

*Department of Nuclear and Quantum Engineering, KAIST, 291 Daehak-ro, Yuseong, Daejeon 305-701, Republic of Korea*
(Received April 29, 2014; Revised April 29, 2014; Accepted April 29, 2014)

The isothermal corrosion tests of several types of stainless steels, Ni-based alloys, and ferritic-martensitic steels (FMS) were carried out at the temperature of 550 and 650 °C in SFR S-CO$_2$ environment (200 bar) for 1000 h. The weight gain was greater in the order of FMSs, stainless steels, and Ni-based alloys. For the FMSs (Fe-based with low Cr content), a thick outer Fe oxide, a middle (Fe,Cr)-rich oxide, and an inner (Cr,Fe)-rich oxide were formed. They showed significant weight gains at both 550 and 650 °C. In the case of austenitic stainless steels (Fe-based) such as SS 316H and 316LN (18 wt.% Cr), the corrosion resistance was dependent on test temperatures except SS 310S (25 wt.% Cr). After corrosion test at 650 °C, a large increase in weight gain was observed with the formation of outer thick Fe oxide and inner (Cr,Fe)-rich oxide. However, at 550 °C, a thin Cr-rich oxide was mainly developed along with partially distributed small and nodular shaped Fe oxides. Meanwhile, for the Ni-based alloys (16-28 wt.% Cr), a very thin Cr-rich oxide was developed at both test temperatures. The superior corrosion resistance of high Cr or Ni-based alloys in the high temperature S-CO$_2$ environment was attributed to the formation of thin Cr-rich oxide on the surface of the materials.

Keywords : *super-critical CO$_2$, stainless steel, weight gain, corrosion resistance*

## 1. Introduction

A super-critical CO$_2$ (S-CO$_2$) Brayton cycle has been considered as one of the promising energy conversion systems of sodium-cooled fast reactor (SFR) which could replace the steam Rankine cycle.[1] By applying S-CO$_2$ cycle to SFR (or, SFR S-CO$_2$), the inherent safety could be improved by alleviating the concern of explosive reaction between liquid sodium and high temperature steam. In addition, an increase in thermal efficiency of the system would be achieved at the operating temperature range of 500-550 °C.[2] Meanwhile, corrosion behaviors of candidate materials for the intermediate heat exchanger (IHX) should be evaluated because the poor corrosion resistance (thick oxide) might deteriorate the heat transfer capability, resulting in decrease in the thermal efficiency as well as the loss of integrity of the IHX. Previously, corrosion characteristics of materials in CO$_2$ had been studied for CO$_2$-cooled advanced gas reactors (AGR) applications.[3] However, because of different operating conditions (max. 650 °C and 4 MPa) as well as limited materials used in AGR, those results could only limited application to the anticipated SFR S-CO$_2$ environments (500-550 °C and 20 MPa).

Corrosion behaviors of several types of stainless steels, Ni-based alloys, and ferritic-martensitic steels have been investigated for SFR S-CO$_2$ application since the late 2000s. Most of previous studies focused on the accelerated corrosion behaviors by increasing testing temperature to 600-650 °C[4,5] from 500-550 °C (an actual anticipated SFR operating temperature) to assess the long-term behaviors in short period of time.[6,7] However, there is a concern that the mechanisms of corrosion and materials degradation could be altered by raising the test temperature too much from the operating condition. Therefore, in this study, corrosion test of candidate structural materials in S-CO$_2$ environment was carried out for up to 1000 h at two temperatures (550 vs. 650 °C) which represented the operating and accelerated test conditions, respectively. Effects of S-CO2 temperatures as well as CO2 pressures (200 bar vs. atmospheric pressure) on corrosion resistance of candidate materials were investigated. Finally, the corrosion resistance of candidate materials was discussed in view of the type of matrix elements (Fe or Ni) and Cr contents (9-28 wt.% Cr).

---

[†] Corresponding author: chjang@kaist.ac.kr

**Table 1. Chemical compositions of structural materials in the corrosion test (in wt.%)**

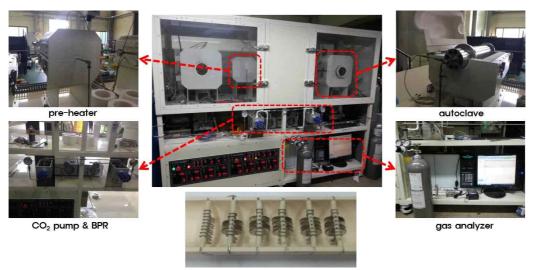|  | Fe | Cr | Ni | C | Ti | Mo | Mn | Al | Si | Cu | Etc. |
|---|---|---|---|---|---|---|---|---|---|---|---|
| SS 310S | Bal. | 24.7 | 19.1 | .06 | - | - | .8 | - | .6 | - | - |
| SS 316H | Bal. | 17.3 | 10.7 | .05 | - | 2.1 | .6 | - | .6 | .2 | Co : .16 |
| SS 316LN | Bal. | 18.9 | 13.9 | .03 | - | - | 1.9 | - | .6 | - | N : .16 |
| SS 347H | Bal. | 18.3 | 8.6 | .07 | - | - | 1.2 | - | .6 | - | Nb : .43 |
| Inconel 600 | 9.33 | 16.1 | Bal. | .08 | .20 | - | .3 | .16 | .3 | .02 | B : .002 |
| Inconel 690 | 8.3 | 28.4 | Bal. | .02 | .3 | - | .2 | .3 | .2 | .01 | B : .002 Nb < .01 |
| Incoloy 800HT | Bal. | 21.0 | 33.6 | .06 | .55 | 0.2 | .9 | .48 | .4 | .1 | B : .003 Co : .05 |
| 9Cr FMS | Bal. | 9.3 | 0.1 | .085 | - | 0.9 | .3 | .03 | .3 |  | Nb : .08 |
| 12Cr FMS | Bal. | 12.0 | 0.4 | .19 | - | 1.0 | .4 | - | .1 |  | V : .30 Nb : .02 |



**Fig. 1.** Corrosion test facility for S-$CO_2$ environment.

## 2. Experimental

### 2.1 Test Materials

Nine different materials used in the corrosion tests are listed in Table 1. It can be divided into three types of alloys such as austenitic stainless steels (SS 310S, SS 316H, 316LN, and SS 347H), Ni-base alloys (Inconel 600, Inconel 690, and Incoloy 800HT), and ferritic-martensitic steels (9Cr and 12Cr FMS). Those materials are generally known to have a high strength at the temperature range of 500 - 550 °C. Materials were cut to coupon type specimens of 12 mm in diameter with a hole drilled at the upper part of the specimen to hang it using a Pt wire. In the tests, two samples of each material were used.

### 2.2 Corrosion test

For the high temperature corrosion test in S-$CO_2$ environment, high purity (99.999%) $CO_2$ was used. Fig. 1 shows the S-$CO_2$ corrosion test facility which can be operated at up to 700 °C and 250 bar. Two independent Alloy 625 autoclaves with three zone main heaters were connected to the gas loop. The impurity levels in the test gas were measured at the outlet of the test system using a gas analyzer and a dew point transmitter. Before heating up the furnace, the system was purged with $CO_2$ until the amount of impurities was reduced to a required level. Liquid $CO_2$ was supplied at a constant flow rate of 5 ml/min by $CO_2$ pump supplies, then pre- and main-heaters
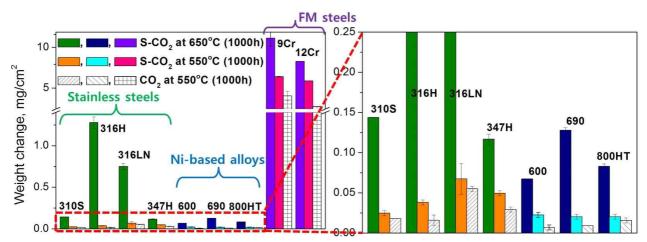
**Fig. 2.** Results of weight gain after exposure in S-CO₂ and CO₂ at 550 and 650 ℃ for 1000 h.
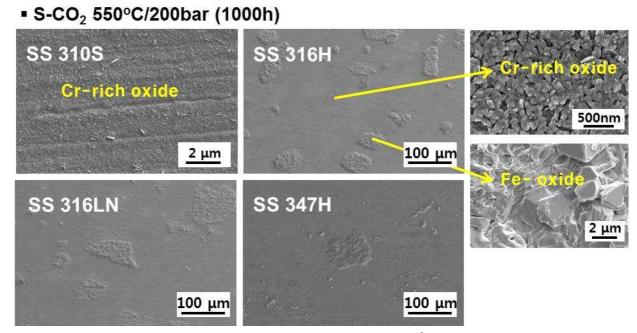


**Fig. 3.** Surface oxide morphology of stainless steels after corrosion tests at 550 ℃ in S-CO₂ (200 bar) for 1000 h.

were used to raise the temperature to the target test temperature at 5 °C/min heating rate.

The isothermal corrosion tests were performed at 550 and 650 °C in S-CO₂ environment of 200 bar up to 1000 h. After the tests, specimens were furnace cooled to room temperature and the pressure was decreased by a back pressure regulator before the specimens were removed for measurement. The weight change was measured for two specimens of each material using a microbalance with a resolution of 0.001 mg. Then one of the samples was selected for the subsequent analyses using scanning electron microscope (SEM) with energy dispersive spectroscopy (EDS).

## 3. Results and Discussion

### 3.1 Corrosion resistance

Fig. 2 shows the results of the weight gain after corrosion test in S-CO₂ environment (200 bar) at 550 and 650 °C for 1000 h. The weight gains of specimens exposed in CO₂ (atmosphere pressure) at 550 °C for 1000 h are also plotted for a comparison. The increase in weight gains was greater in the order of FMSs, stainless steels, and Ni-based alloys in all test conditions. The weight gains in S-CO₂ environment at 650 °C were significantly larger than those at 550 °C. Meanwhile, the weight gains at low CO₂ pressure was smaller than those at high pressure CO₂
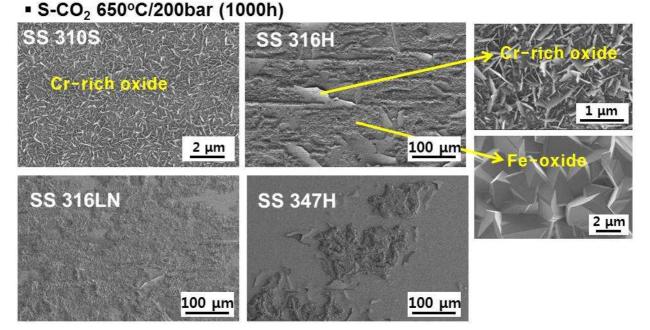
**Fig. 4.** Surface oxide morphology of stainless steels after corrosion tests at 650 $^o$C in S-CO$_2$ (200 bar) for 1000 h.

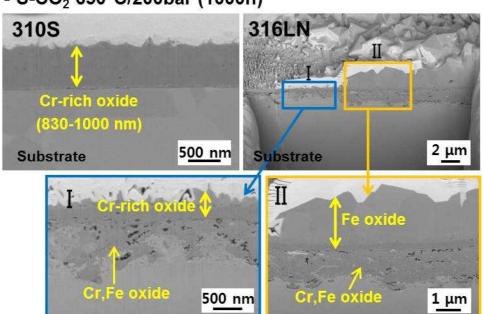(S-CO$_2$) environment, though the differences were rather small.

Based on the weight gain results, three types of corrosion behaviors were observed. First, FMSs (Fe- based alloys with 9 or 12 wt.% Cr) showed the large increase in weigh gains compared to other test materials at both temperatures of 550 and 650 $^o$C. However, in the case of stainless steels (Fe-based alloys with 18-26 wt.% Cr), SS 316H and SS 316LN showed significant difference of weight gain depending on test temperatures between 550 and 650 $^o$C while the difference was relatively small for SS 310S and SS 347H. For Ni-based alloys such as Inconel 600, Inconel 690, and Incoloy 800HT, the weight gains were quite low at both temperatures. Although all of the stainless steels and Ni-based alloys had similar tendency of weight gain after exposure in S-CO$_2$ at 550 $^o$C, the difference between stainless steels and Ni-based alloys became significant at 650 $^o$C. The better corrosion resistance of SS 310S and SS 347H will be described in the following section.

### 3.2 Oxide structure

Figs. 3 and 4 show the surface oxide morphologies of corrosion tested stainless steels in S-CO$_2$ (200 bar) at 550 and 650 $^o$C for 1000 h. The surface oxides consisted of mixture of polygonal shaped Fe oxide and nodular (550 $^o$C) or platelet (650 $^o$C) shaped Cr-rich oxide while the amount of Fe oxide was much greater than Cr-rich oxide at 650 $^o$C except SS 347 H (Fig. 4). It is well understood

that corrosion resistance of SS 347H is better than SS 316 in spite of similar Cr content because of smaller grain size and the presence of 0.43 wt.% of Nb. [8] However, in the case of SS 310S (Fe-based alloy with 25 wt.% Cr), the surface oxide morphology was quite uniform and it is composed of Cr-rich oxide (Cr$_2$O$_3$) without Fe oxide at both temperatures. Fig. 5 shows the representative cross-sectional oxide images of SS 310S and SS 316LN corroded in S-CO$_2$ at 650 $^o$C for 1000 h. As shown in the figures, the thickness of Cr–rich oxide in SS 310S was less than 1 μm whereas in SS 316LN an outer Fe oxide and inner (Cr,Fe)-rich oxide reached up to a few μm. It seems that the large amount of an outer Fe oxide and inner (Cr,Fe) oxide in 316H and 316LN would cause significant increase in weight gains after exposure to S-CO$_2$ at 650 $^o$C. Therefore, it can be thought that high Cr content in SS 310S contributed the formation of protective Cr-rich oxide, which resulted in high corrosion resistance.

Moreover, Ni-based alloys, Inconel 600 (16 wt.% Cr), Inconel 690 (28 wt.% Cr), and Incoloy 800 HT (21 wt.% Cr), showed a high corrosion resistance in S-CO$_2$ at both temperatures. For those alloys, the oxide structure was similar to SS 310S, such that the formation of Cr-rich oxide was mainly observed without Ni oxide as shown in Fig. 6. Although Ni-spinel oxides were observed in 800HT and Alloy 625 previously[9], the amount was very small compared to Cr-rich oxide. According to the Ellingham diagram, the oxygen partial pressure for the

**Fig. 5.** Cross-sectional oxide of SS 310S and SS 316LN after corrosion test at 650 $^{o}$C in S-CO₂ (200 bar) for 1000 h.
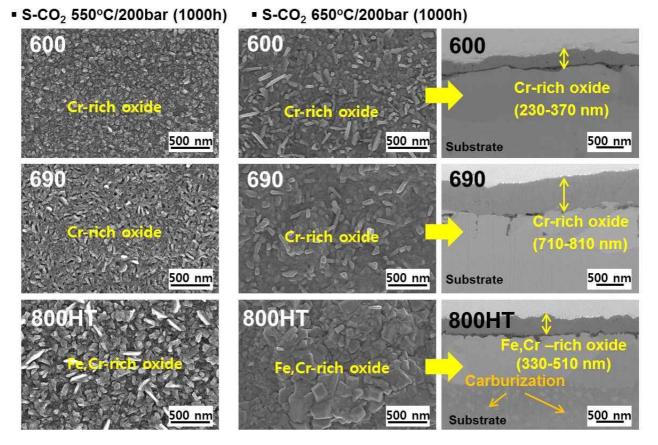


**Fig. 6.** Surface oxide morphology and cross-sectional images of Ni-based alloys after corrosion tests at 550 and 650 $^{o}$C in S-CO₂ (200 bar) for 1000 h.

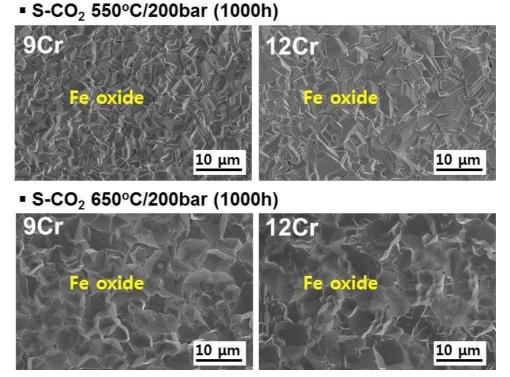**Fig. 7.** Surface oxide morphology of FMS after corrosion tests at 550 and 650 $^{o}$C in S-CO$_2$ (200 bar) for 1000 h.

formation of Ni oxide was higher than Fe oxide and Cr oxide at the temperature range of 550 and 650 $^{o}$C. Therefore, in S-CO$_2$ environment, Ni-based alloys would have a better corrosion resistance than Fe-based alloys by forming protective Cr-rich oxide. Furthermore, in case of the Cr-rich oxide forming alloys, oxide structures were less dependent on temperature while weight gains significantly increased at higher temperature.

For FMS alloys (9 and 12 Cr FMS), the weight gain was exceptionally large compared to stainless steels and Ni-based alloys (Fig.2). A polygonal shaped Fe oxide uniformly covered the outer layer at both temperatures as shown in Fig. 7. Unlike high-Cr stainless steels and Ni-base alloys, relatively low Cr content in FMS was not enough to form protective Cr-rich oxide, which resulted in worst corrosion resistance among the test materials.

As mentioned above, our test results indicate that the oxide structures at 550 $^{o}$C are quite different from those at 650 $^{o}$C. Meanwhile, Furukawa et al.[7] also observed partial nodular shape oxides formed on SS 316FR 1000 h exposed in S-CO2 (20 MPa) at 600 $^{o}$C. Therefore, it is considered that for the stainless steels containing about 18 wt.% Cr, accelerated test condition of 650 $^{o}$C seems too high to assess corrosion behaviors in S-CO2 environment for the SFR application (around 500 - 550 $^{o}$C). However, for the other materials such as SS 310S,

Ni-based alloys, and FMSs, similar oxide structures were developed at 550 and 650 $^{o}$C, which suggest that corrosion behaviors are similar at both temperatures.

## 4. Conclusions

A corrosion resistance of structural materials in super-critical CO$_2$ was studied for the application in the SFR S-CO$_2$ environment. Isothermal corrosion tests of eight materials were carried out in S-CO$_2$ environment (200 bar) at 550 and 650 $^{o}$C up to 1000 h. Based on the test and subsequent analyses, the following conclusions were drawn about the corrosion resistance of structural materials in S-CO$_2$ environments.

1. The weight gain was greater in the order of FMSs, stainless steels, and Ni-based alloys in all test conditions.
2. FMSs (Fe-based alloys with 9 or 12 wt.% Cr) showed the poor corrosion resistance even at the temperature of 550 $^{o}$C by forming an thick outer Fe oxide, a middle (Fe,Cr)-rich oxide, and an inner (Cr,Fe)-rich oxide layer. The relatively low Cr content in FMS was not enough to form protective Cr-rich oxide in test environments.
3. In the case of stainless steels (Fe-based alloys with 18-26 wt.% Cr), the surface oxides consisted of mixture of polygonal shaped Fe oxide and nodular (550 $^{o}$C)

or platelet (650 °C) shaped Cr-rich oxide. The amount of Fe oxide became much greater than that of Cr-rich oxide at 650 °C. At the test temperature of 650 °C, a large increase in the weight gains of SS 316H and SS 316LN were attributed to the extensive formation of thick outer Fe oxide and inner Cr,Fe-rich oxide.

4. The superior corrosion resistance of high Cr stainless steels and Ni-based alloys in S-CO₂ environments up to 650 °C was attributed to the formation of thin protective Cr-rich oxide.

## Acknowledgments

## References

1. Y. I. Chang, P. J. Finck, C. Grandy, Argonne National Laboratory report ANL-ABR-1 (ANL-AFCL-173) (2006).
2. V. Dostal M.J. Driscoll, P. Hejzlar, MIT Annual and Progress Reports, MIT-ANP-TR-100 (2004).
3. D. J. Beech, R. May, OECD Proceedings, the First Information Exchange Meeting on Basic Studies on High-Temperature Engineering, Paris, France (1999).
4. G. Cao, V. Firouzdor, K. Sridharan, M. Anderson, T.R. Allen, Corros. Sci., **60,** 246 (2012).
5. K. Sridharan, M. Anderson, G. Cao, J. Jelinek, V. Firouzdor, T.R. Allen, Supercritical CO₂ Power Cycle Symposium, May 24-25, Boulder, Colorado (2011).
6. F. Rouillard, F. Charton, G. Moine, Supercritical CO₂ Power Cycle Symposium, April 29-30, Troy, NY (2009).
7. T. Furukawa, Y. Inagaki, M. Aritomi, Progress in Nuclear Energy, **53**, 1050 (2011).
8. S. Kihara, A. Ohtomo, I. Kajigaya, F. Kishimoto, Materials and Corrosion, **39,** 69 (1988).
9. M. Anderson, Project Report of Nuclear Energy University Program 09-778, University of Wisconsin (2012).